

Gamma-ray and neutrino flares produced by protons accelerated on an accretion disk surface in AGN

W. Bednarek^{1,2} and R.J. Protheroe¹

¹*Department of Physics and Mathematical Physics, The University of Adelaide, Adelaide, Australia 5005.*

²*Department of Experimental Physics, University of Łódź, 90-236 Łódź, ul. Pomorska 149/153, Poland.*

Accepted 199 Received 199; in original form 1998

ABSTRACT

We discuss the consequences of almost rectilinear acceleration of protons to extremely high energies in a reconnection region on the surface of an accretion disk which surrounds a central black hole in an active galaxy. The protons produce γ -rays and neutrinos in interactions with the disk radiation as considered in several previous papers. However, in this model the secondary γ -rays can initiate cascades in the magnetic and radiation fields above the disk. We compute the spectra of γ -rays and neutrinos emerging from regions close to the disk surface. Depending on the parameters of the reconnection regions, this model predicts the appearance of γ -ray and neutrino flares if protons takes most of the energy from the reconnection region. In contrast, if leptons take most of the energy, they produce pure γ -ray flares. The γ -ray spectrum expected in the case of hadronic cascading is compared with the spectrum observed during the flare in June 1991 from 3C 279. The neutrino flares which should accompany these gamma-ray flares may be detected by future large scale neutrino telescopes sensitive at $\sim 10^5$ TeV.

Key words: galaxies: active – quasars: jets – radiation mechanisms: gamma rays – galaxies: individual: 3 C279

1 INTRODUCTION

Flares on very short time scales in TeV γ -rays have been recently detected from Mrk 421, Mrk 501, and 1ES2344+514 (e.g. Buckley et al. 1996, Gaidos et al. 1996, Aharonian et al. 1997, Catanese et al. 1998) and in the EGRET energy range from many other blazars (e.g. von Montigny et al. 1995, Mattox et al. 1997). Flares observed with a ~ 1 day time scale are usually interpreted in terms of a relativistic shock moving through the jet with a Lorentz factor of the order of ~ 10 (e.g. Maraschi, Ghisellini & Celloti 1992, Mannheim & Biermann 1992, Dermer & Schlickeiser 1993, Bednarek 1993, Sikora, Begelman & Rees 1994, Blandford & Levinson 1995, Ghisellini & Madau 1996, Protheroe 1997). However, the production of such flares may also be a natural consequence of energization of particles in a way similar to that causing solar flares, but in this case occurring in regions of magnetic reconnection which may exist on the disk surface (Haswell, Tajima & Sakai 1992, Lesch & Pohl 1992). Reconnection of magnetic field may also occur in the jet (e.g. Romanova & Lovelace 1992, Bisnovaty-Kogan & Lovelace 1995). The processes of γ -ray production by leptons accelerated in electric fields generated in the jet has been recently discussed by Bednarek & Kirk (1995,

henceforth BK95) and Bednarek, Kirk & Mastichiadis (1996, henceforth BKM96).

The acceleration of particles by almost rectilinear electric fields has some advantages in comparison to the stochastic acceleration by a relativistic shock since, in principle, particles can reach very high energies on shorter time scales. However, the process of reconnection of magnetic fields in astrophysical environments is poorly understood. Recently, Haswell, Tajima & Sakai (1992) have developed a model of explosive reconnection of magnetic fields on the surface of an accretion disk. They argued that particles (electrons, protons) can be accelerated to extremely high energies ($\sim 10^{20-21}$ eV). The consequences of this model for γ -ray production in blazars has been investigated recently by Bednarek (1997, henceforth B97), assuming that accelerated leptons develop cascades in the magnetic field through production of γ -rays by the synchrotron process, and by the creation of secondary pairs by γ -rays in the magnetic field. The γ -ray spectra, emerging from a region on the inner part of an accretion disk around a massive black hole, are in agreement with observations of blazars.

In this paper, we discuss the consequences of acceleration of protons in almost uniform electric fields induced by magnetic reconnection on the disk surface. Protons accel-

arXiv:astro-ph/9802288v1 23 Feb 1998

ated to extremely high energies produce γ -rays and neutrinos through the decay of pions produced in collisions with disk photons. Neutrinos freely escape, but γ -ray photons initiate cascades in the magnetic and radiation fields above the disk (B97). The conditions for acceleration of protons, and their propagation in the disk radiation, are discussed in Sect. 2.1 and 2.2. We compute the spectra of neutrinos and γ -rays (Sect. 2.3), and describe the details of the cascades initiated by these γ -rays (Sect. 3). Example γ -ray spectra are compared with observations of the June 1991 flare from 3C 279, and a prediction of the neutrino emission accompanying this flare is given in Sect. 4.

2 ACCELERATION OF PROTONS DURING EXPLOSIVE RECONNECTION IN THE INNER PART OF AN ACCRETION DISK

We make use of the model of Haswell et al. (1992) in which particles can be accelerated to extremely high energies during explosive reconnection of the magnetic field on the surface of an accretion disk in the central parts of active galactic nuclei (AGN). Let us assume that reconnection of the magnetic field occurs over a distance l_{rec} somewhere in the inner part of the optically thick accretion disk. The local radiation field in this region can be described by a black body spectrum with temperature T . The induced electric field strength E_f can be estimated as $E_f \cong cB$, where B is the reconnecting magnetic field strength and c is the velocity of light. Then, the maximum possible energies, which can be reached by particles (in eV), are

$$E_p = E_f l_{\text{rec}} \approx 3 \times 10^{18} B_5 l_{11}, \quad (1)$$

where $B = 10^5 B_5$ G, $l_{\text{rec}} = 10^{11} l_{11}$ cm.

2.1 Conditions for acceleration of protons

Protons accelerated in the electric field lose energy by e^\pm pair and pion production in collisions with the black body photons after reaching the thresholds for these reactions. Since the threshold for e^\pm pair production is about two orders of magnitude lower than that for pion production, e^\pm pairs are first injected into the electric field in the reconnection region. The characteristic distance scale $\lambda_{p\gamma e^\pm}$ (in cm), for this process to occur efficiently, can be estimated by

$$\lambda_{p\gamma e^\pm} \approx (\sigma_{p\gamma \rightarrow e^\pm} n_{\text{bb}})^{-1} \approx 5.1 \times 10^{12} T_4^{-3}, \quad (2)$$

where $\sigma_{p\gamma \rightarrow e^\pm} \approx 10^{-26}$ cm² is the cross section for e^\pm pair production in collisions of protons with photons (Maximon 1968, Chodorowski, Zdziarski & Sikora 1992), n_{bb} is density of the black body photons, and the local disk temperature in the reconnection region is expressed in units of $T_4 = T/10^4$ K. We shall show later that this process is not an important energy loss mechanism for accelerated protons since its inelasticity coefficient is small ($\sim 2 \times 10^{-3}$). Nevertheless, the injected secondary e^\pm pairs can initiate inverse Compton e^\pm pair cascades in the disk radiation and the electric field of the reconnection region (BK95). The products of such a cascade can saturate the external electric field if the length of the reconnection region is longer than (BK95)

$$\lambda_{\text{sat}} \approx 100 \lambda_{\text{trip}} \approx 3.85 \times 10^{14} T_4^{-3}, \quad (3)$$

where $\lambda_{\text{trip}} \approx (\sigma_{\text{trip}} n_{\text{bb}})^{-1}$ is characteristic distance scale for the triplet e^\pm pair production by electrons in collision with soft photons, and $\sigma_{\text{trip}} \approx \sigma_T/50$ (Mastichiadis 1991), σ_T is the Thomson cross section. In this case, most of the energy extracted from the electric field is transferred to secondary e^\pm pairs if

$$l_{\text{rec}} > \lambda_{\text{sat}}. \quad (4)$$

Eq. 4 can be written as a condition on the temperature of the black body radiation in the reconnection region such that the electric field is saturated,

$$T_4 > T_{4,\text{tr}} \approx 15.7 l_{11}^{-1/3}. \quad (5)$$

If the temperature of the black body radiation is lower than $T_{4,\text{tr}}$ then the reconnection energy can efficiently accelerate relativistic protons. These protons can then produce pions in interactions with the disk radiation both during the acceleration stage and after emerging from the reconnection region, provided that the electric field is strong enough to allow them to reach energies, $E_{p,\text{min}}$ (in eV), above the threshold for pion production,

$$E_p > E_{p,\text{min}} \cong 3 \times 10^{16} T_4^{-1}. \quad (6)$$

The characteristic distance scale for pion production by protons can be estimated by,

$$\lambda_{p\gamma\pi} \approx (\sigma_{p\gamma\pi} n_{\text{bb}})^{-1} \approx 1.7 \times 10^{14} T_4^{-3} \quad (7)$$

where $\sigma_{p\gamma\pi} \approx 3 \times 10^{-28}$ cm² is the cross section for pion production in collisions of protons with photons (Stecker 1968). Comparison of $\lambda_{p\gamma\pi}$ with the characteristic distance scale of the reconnection region, which is the inner radius of an accretion disk r_{in} , allows us to estimate the parameters of the accretion disk for which the proton energy losses by pion production become significant. We find that the minimum local disk temperature in the reconnection region depends on the characteristic disk dimension,

$$T_4 > 1.2 r_{14}^{-1/3}, \quad (8)$$

where $r_{\text{in}} = 10^{14} r_{14}$ cm.

The maximum proton energies, estimated using Eq. 1, can be expressed in terms of the temperature of the black body radiation in the reconnection region if we use the common assumption of equipartition of the magnetic and radiation energy densities close to the accretion disk. However, we note that Haswell, Tajima & Sakai (1992) argue that the magnetic field in the inner disk can be significantly amplified as a result of its differential rotation from the values close to the equipartition ($B_{\text{eq}} \approx 40 T_4^2$) up to values of the order of $B \approx 300 B_{\text{eq}}$. In such a case, the formula for the proton energy (Eq. 1) can be rewritten in the form

$$E_p \approx 3.6 \times 10^{17} T_4^2 l_{11}. \quad (9)$$

Since efficient proton acceleration requires the electric field not to be saturated by pairs, the disk temperature in the reconnection region cannot exceed that given by Eq. 5, and we can express the maximum possible proton energy (in eV) in terms of the local disk temperature

$$E_{p,\text{max}} \approx 1.4 \times 10^{21} T_4^{-1}. \quad (10)$$

The assumption of equipartition between the primary magnetic field energy density and the radiation energy density

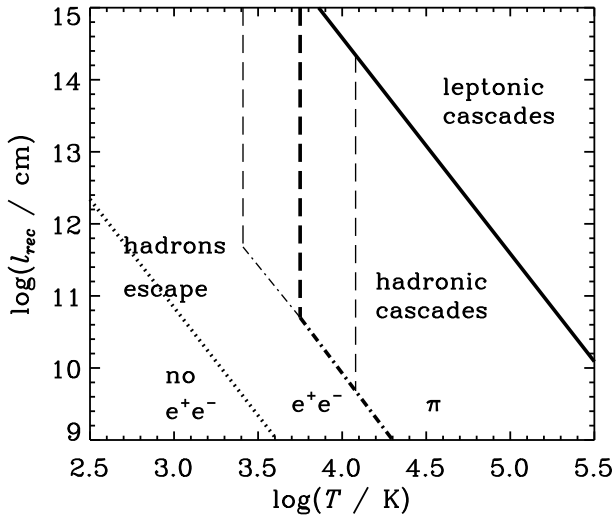


Figure 1. The conditions for cascading initiated in the radiation field of the accretion disk by hadrons accelerated on the disk surface. For the parameters in the areas marked by ‘hadrons escape’, the protons escape from the radiation of the disk without significant energy losses. In the area ‘no e^+e^- ’ they have energies below the threshold for e^\pm pair production and in the area ‘ e^+e^- ’, they inject e^\pm pairs. For parameters in the area marked by ‘hadronic cascades’, protons efficiently lose energy on pion production and the pion decay products initiate cascades in the magnetic and radiation fields. In the area ‘leptonic cascades’, the energy of the electric field is extracted mainly by secondary leptons which initiate cascades in the magnetic and radiation fields (Eq. 5). The thick long-dashed line shows the limit for efficient extraction of energy from hadrons (Eq. 8) for a disk inner radius of $r_{\text{in}} = 10^{15}$ cm, and the thin long-dashed lines give the limits for $r_{\text{in}} = 10^{14}$ cm (right) and 10^{16} cm (left).

allows us to derive the minimum length (in cm) of the reconnection region for which accelerated protons can reach energies above the thresholds for e^\pm pair production and pion production (Eq. 6) giving

$$l_{\text{rec}}^{e^\pm} > 6.9 \times 10^7 T_4^{-3}, \quad (11)$$

and

$$l_{\text{rec}}^\pi > 8.3 \times 10^9 T_4^{-3}, \quad (12)$$

in cm, respectively. The conditions for acceleration and propagation of protons (Eqs. 5, 8, 11, and 12) allow us to distinguish three interesting scenarios which can be separated in the parameter space (shown in Fig. 1) defined by the length of the acceleration region l_{rec} and the temperature of the local black body radiation T . For the regions labeled by ‘hadrons escape’, the proton energy losses during acceleration and subsequent propagation in the disk radiation are negligible, allowing protons to leave the accretion disk with very high energies. If the acceleration distance is high enough, the protons can reach the threshold for e^\pm pair production, injecting a few secondary pairs (area marked by ‘ e^+e^- ’, between the dot-dashed line (Eq. 12), dotted line (Eq. 11) and long-dashed line (Eq. 8)). Below the dotted line, protons do not inject pairs (area marked by ‘no e^+e^- ’). If protons reach the threshold for pion production (Eq. 12, marked by the dot-dashed line), they suffer strong energy losses. The proton energy losses becomes significant for disk

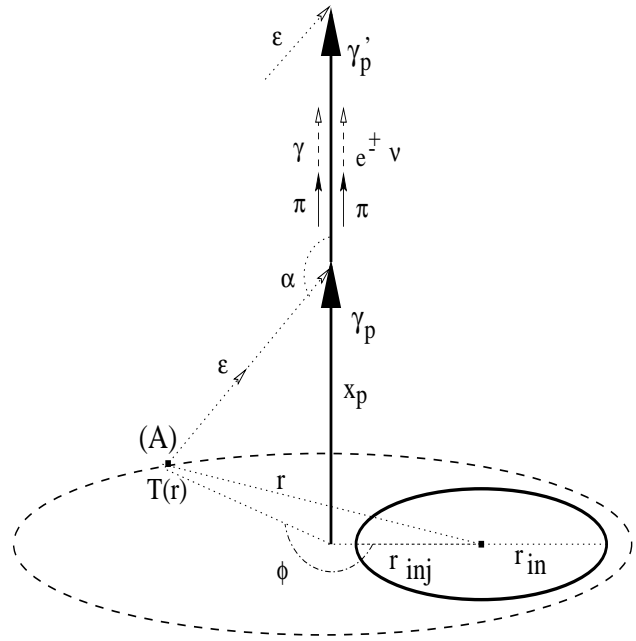


Figure 2. Schematic representation of the scenario discussed in this paper. Relativistic protons with Lorentz factors γ_p are injected at a reconnection region which is at a distance r_{inj} from the center of the disk. A proton interacts at height x_p with a soft photon from the disk, having energy ϵ , emitted at point A on the disk defined by the angles α and ϕ . The energy ϵ is determined by the local disk temperature $T(r)$ at point A. As a result, pions are produced which decay into γ -rays, e^\pm pairs, and neutrinos. The surviving proton, with the Lorentz factor $\gamma_{p'}$, may again interact at some distance from the disk.

temperatures above the values estimated by Eq. 8 (marked by the long-dashed lines for different disk inner radii). In the area marked by ‘hadronic cascades’, the initial proton’s energy is transferred to pions whose decay products (leptons, photons) initiate cascades in the magnetic and radiation fields above the disk. In the present paper, we shall concentrate on this case. In the last area, marked by ‘leptonic cascades’, the production of e^\pm pairs by protons and subsequently by these pairs in the inverse Compton e^\pm pair cascade developing in the electric field, is very efficient, even during the acceleration stage in the reconnection region. These secondary e^\pm pairs may even saturate the electric field (BK95). Most of the energy of the electric field is then transferred to leptons (and γ -rays) which initiate cascades in the magnetic and radiation fields above the disk identical to those initiated by primary leptons (B97). Note that the processes occurring for the parameters in the area ‘hadronic cascades’ turn out to be the production of γ -ray and very high energy neutrino flares, whereas for the processes occurring for parameters in the area ‘leptonic cascades’ only γ -ray flares are produced.

2.2 Propagation of relativistic protons in the disk radiation

The protons, escaping from the reconnection region with energies estimated by Eq. (9) or (10), produce pions in col-

lisions with the disk photons on a characteristic distance scale given by Eq. (7). We simulate propagation of protons through the anisotropic disk radiation by using the Monte Carlo method. It is assumed that protons are injected on the surface of a thin disk at the distance r_{inj} from its center (see Fig. 2). We consider a simple disk model in which the disk emits black body radiation with characteristic temperature depending on the distance from the disk center according to the model of Shakura & Sunyaev (1973). Therefore, the disk radiation is defined by the disk inner radius r_{in} and its temperature T_{in} at r_{in} .

In order to simulate the propagation of protons and the production of γ -rays and neutrinos, we first determine the point of interaction of the proton with a soft photon coming from the disk. The interaction length, $\lambda_{p\gamma\pi}$, for the proton in the disk radiation, as a function of its energy E_p (Lorentz factor γ_p and velocity β_p) and its distance, x , from the disk surface is calculated, by integrating the formula

$$\lambda_{p\gamma\pi}^{-1}(E_p, x) = \int \int n(\epsilon, \Omega) \sigma_{p\gamma\pi}(\epsilon') \frac{\epsilon'}{\epsilon} d\epsilon d\Omega, \quad (13)$$

where $n(\epsilon, \Omega)$ is the differential density of photons emitted by the disk, $\sigma_{p\gamma\pi}(\epsilon')$ is the energy dependent cross section for pion production in proton–photon collision (Stecker 1968), $d\Omega = d\phi d\mu$ is the solid angle of incident disk photons, $\mu = \cos \alpha$ (see Fig. 2), $\epsilon' = \epsilon \gamma_p (1 + \beta_p \mu)$ and ϵ are energies of soft photons in the proton and LAB frames, respectively. To find out if protons have a chance to interact with the disk photons for specific disk parameters, the optical depth for protons is obtained by integrating along the proton path

$$\tau_{p\gamma\pi} = \int_0^\infty \lambda_{p\gamma\pi}^{-1}(E_p, x) dx. \quad (14)$$

The optical depth for protons is shown in Fig. 3a as a function of proton energy, and for different parameters of the disk radiation, r_{in} and T_{in} . It is clear that for the disk parameters expected in AGNs protons have a significant probability of interacting, and may even undergo multiple interactions. In order to find out if the competing process of e^\pm pair production may become an important energy loss mechanism for protons, we calculate the energy loss rates in the disk radiation for e^\pm pair production at a fixed distance, x , from the disk surface

$$\frac{dE_p(x)}{dx} = \int \int n(\epsilon, \Omega) \sigma_{p\gamma e^\pm}(\epsilon') K(\epsilon') \frac{\epsilon'}{\epsilon} d\epsilon d\Omega, \quad (15)$$

where the cross section for e^\pm pair production, $\sigma_{p\gamma e^\pm}(\epsilon')$, and the inelasticity $K(\epsilon')$ are taken from Chodorowski, Zdziarski & Sikora (1992). The optical depth for the total energy loss by protons during their propagation through the disk radiation from the disk surface to infinity is

$$\tau_{p\gamma e^\pm} = \int_0^\infty \frac{dE_p(x)}{dx} \frac{1}{E_p} dx. \quad (16)$$

This value is plotted in Fig. 3b, for the same disk parameters as used in Fig. 3a. It is evident that proton energy losses on e^\pm pair production are not important except for the case of very large disks with high inner disk temperatures ($r_{\text{in}} > 10^{15}$ cm and $T_{\text{in}} > 10^5$ K). Such disks, with luminosities $L_{\text{disk}} > 7 \times 10^{46}$ erg s $^{-1}$, have not been observed. The blazar 3C 273 has a disk luminosity a factor of

about 3 lower, $L_{\text{disk}} \approx 2 \times 10^{46}$ erg s $^{-1}$ (Lichti et al. 1995), but this seems to be exceptionally high. Therefore, we neglect the influence of e^\pm pair production on the propagation of protons since these losses can be neglected in comparison to pion production losses at energies above $E_{p,\text{min}}$ (Eq. 6). However this process can become important if proton energies drop below the threshold for pion production far from the accretion disk. Such pairs could contribute to the formation of a broad synchrotron bump at low energies observed in blazars.

If protons are very close to the disk, their interaction length does not change significantly with distance x_0 from the disk. Using the Monte Carlo method, the point of interaction of a proton with the disk photon can be then determined from

$$x_p = x_0 - \lambda_{p\gamma\pi} \ln(1 - P_1), \quad (17)$$

where P_1 is a random number. However at larger distances from the disk the radiation becomes anisotropic, and the proton interaction length can change significantly. Then the distance of proton interaction, x_p , is obtained by solving

$$P_1 = \exp\left[-\int_{x_0}^{x_p} \lambda_{p\gamma\pi}(l)^{-1} dl\right] \quad (18)$$

where l is the distance measured along the proton's path. However, if

$$P_1 < \exp\left[-\int_{x_0}^\infty \lambda_{p\gamma\pi}(l)^{-1} dl\right] \quad (19)$$

the proton is assumed to have escaped from the disk radiation. The condition applied in order to distinguish between quasi-isotropic and anisotropic cases is this same as used in Bednarek (B97) (see footnote on page 5 in that paper).

Having selected randomly the distance, x_p , at which proton interacts with a disk photon, we have to sample the cosine angle, μ , of the photon from the disk which interacts with the proton. The possible range of photon directions (from $\mu = -1$ to μ_{max} , which corresponds to the outer disk radius) is divided into one hundred intervals with width $\Delta\mu$, corresponding to annular rings on the accretion disk centered on r_{inj} . The ring defined by $\mu_{\text{ph}}(E_p, x_p)$, from which a disk photon is interacting with the proton, is selected randomly by solving

$$P_2 = \frac{\sum_{-1}^{\mu_{\text{ph}}(E_p, x_p)} \int \int n(\epsilon, \Omega) \sigma_{p\gamma\pi}(\epsilon') \frac{\epsilon'}{\epsilon} d\epsilon d\phi \Delta\mu}{\sum_{-1}^{\mu_{\text{max}}} \int \int n(\epsilon, \Omega) \sigma_{p\gamma\pi}(\epsilon') \frac{\epsilon'}{\epsilon} d\epsilon d\phi \Delta\mu} \quad (20)$$

where P_2 is a random number.

Finally we have to sample the energy of the disk photon coming from the ring μ_{ph} for a proton located at a distance x_p . To save computing time we approximate the black body spectrum of photons emitted at distance r from the disk center by monoenergetic photons with energies corresponding to the mean photon energy of the black body spectrum, $\epsilon = 2.7 k_B T(r)$, where k_B is the Boltzman constant, and $T(r) = T_{\text{in}}(r/r_{\text{in}})^{-3/4}$, as predicted by Shakura & Sunyaev model. In such a case, the energy of photons coming from a specific ring μ_{ph} is uniquely defined by the azimuthal angle ϕ (see Fig. 2). We can sample the angle ϕ randomly by

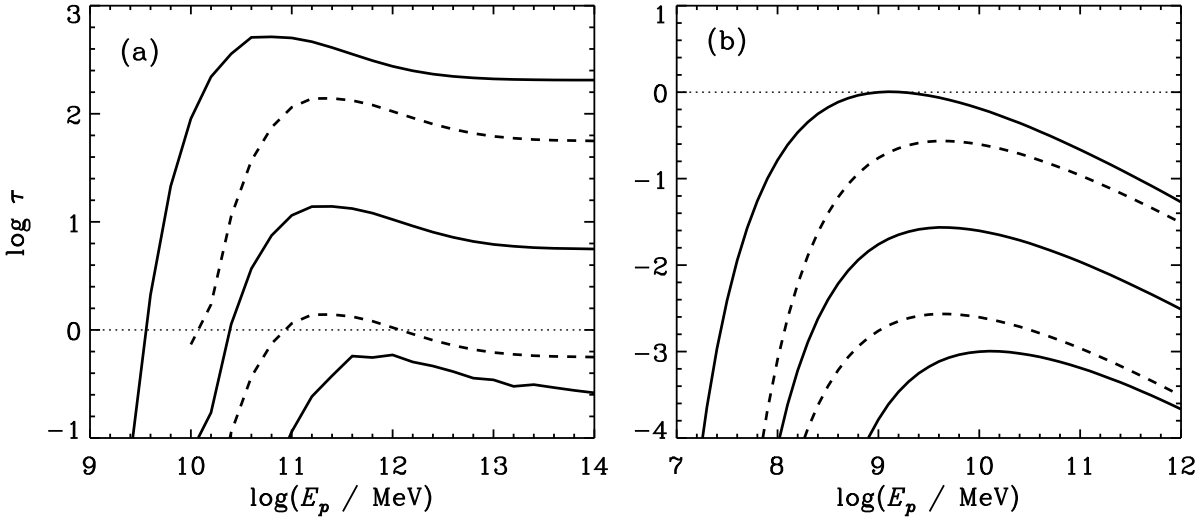


Figure 3. (a) Optical depth for pion production collisions of protons with the disk photons; (b) optical depth for energy loss of protons by production of e^\pm pairs during propagation. The full curves show the results for disk inner radius $r_{\text{in}} = 10^{15}$ cm and different inner disk temperatures: $T_{\text{in}} = 10^4$ (bottom), 3×10^4 , and 10^5 K (top); the dashed curves are for $T_{\text{in}} = 3 \times 10^4$ K and different inner disk radii: $r_{\text{in}} = 10^{14}$ (bottom), and 10^{16} cm (top).

solving

$$P_3 = \frac{\int_{\phi_{\text{min}}}^{\phi_\epsilon} n(\epsilon(\phi), \mu) \sigma_{p\gamma\pi}(\epsilon') \frac{\epsilon'}{\epsilon} d\phi}{\int_{\phi_{\text{min}}}^{\pi} n(\epsilon(\phi), \mu) \sigma_{p\gamma\pi}(\epsilon') \frac{\epsilon'}{\epsilon} d\phi} \quad (21)$$

where P_3 is a random number and ϕ_{min} is equal to 0, or is calculated for the given inner disk radius r_{in} if the ring defined by μ lies partially inside r_{in} . The interacting photon is now completely specified, allowing us to compute its energy in the proton frame $\epsilon' = \epsilon(\phi_\epsilon) \gamma_p (1 + \beta_p \mu_{\text{ph}})$, model the interaction, and obtain the energies of pions produced in the proton frame.

The above procedure is repeated until the relativistic proton escapes from the disk radiation. The parameters of produced pions are stored for further computation of neutrino and γ -ray spectra.

2.3 Spectra of neutrinos and gamma-rays from decay of pions

Because of the complexity of the present model, in particular the cascading in the radiation and magnetic fields, we have had to make a number of approximations in order to save computer time. In particular, in the calculation of spectra of secondary particles produced in interactions of protons with soft photons was, of necessity, subject to approximation. However, we include single pion production (in the Δ resonance region) although in an approximate way, and the effects of multiple pion production far away from the threshold is treated using an average multiplicity relation similar to that found in low energy pp interactions,

$$\langle n_\pi \rangle \propto s^{0.25}, \quad (22)$$

where $s = m_p^2 + 2\epsilon E_p (1 + \beta_p \mu)$ is the center of momentum frame energy squared (in this section we define $c \equiv 1$), and m_p is the proton rest mass. The ratio of charged pions to all

pions produced in a single multiple pion interaction is taken to be $n_{\pi^\pm}/n_\pi \approx 2/3$.

In the case of single pion production (Δ resonance decay) the pion energies in the center of momentum system (CMS) are given by,

$$E_\pi^{\text{CMS}} = \frac{2m_p \epsilon' + m_\pi^2}{2\sqrt{s}}. \quad (23)$$

It is assumed that the Δ resonance decays isotropically, so that pions are produced isotropically in the CMS and we may sample their direction cosine angle using

$$\mu_\pi = 2P_4 - 1, \quad (24)$$

where P_4 is a random number. The energy of the pion in the LAB frame is then

$$E_\pi^{\text{LAB}} = \gamma_{\text{CMS}} (E_\pi^{\text{CMS}} + \beta_{\text{CMS}} p_\pi^{\text{CMS}} \mu_\pi), \quad (25)$$

where $\gamma_{\text{CMS}} = (E_p + \epsilon)/\sqrt{s}$, $\beta_{\text{CMS}} = \sqrt{1 - 1/\gamma_{\text{CMS}}^2}$, and p_π^{CMS} is the pion momentum in the CMS.

The pions decay isotropically in their rest frame producing: γ -rays, muon neutrinos, and muons with energies which we approximate by

$$E_\gamma^\pi = 0.5m_\pi, \quad (26)$$

$$E_\nu^\pi = 0.5(m_\pi^2 - m_\mu^2)/m_\pi, \quad (27)$$

and

$$E_\mu^\pi = 0.5(m_\pi^2 + m_\mu^2)/m_\pi, \quad (28)$$

where m_π is the rest mass of a pion (we neglect the mass difference between neutral and charged pions). The cosine angles of decay products of pions can be sampled randomly from

$$\mu_{\gamma,\nu}^\pi = 2P_5 - 1, \quad (29)$$

where P_5 is a random number, and $\mu_\mu = -\mu_\nu$. Their energies in the LAB frame are given by

$$E_{\gamma,\nu,\mu}^{\text{LAB}} \approx E_{\gamma,\nu,\mu}^\pi \gamma_\pi (1 + \beta_\pi \mu_{\gamma,\nu,\mu}), \quad (30)$$

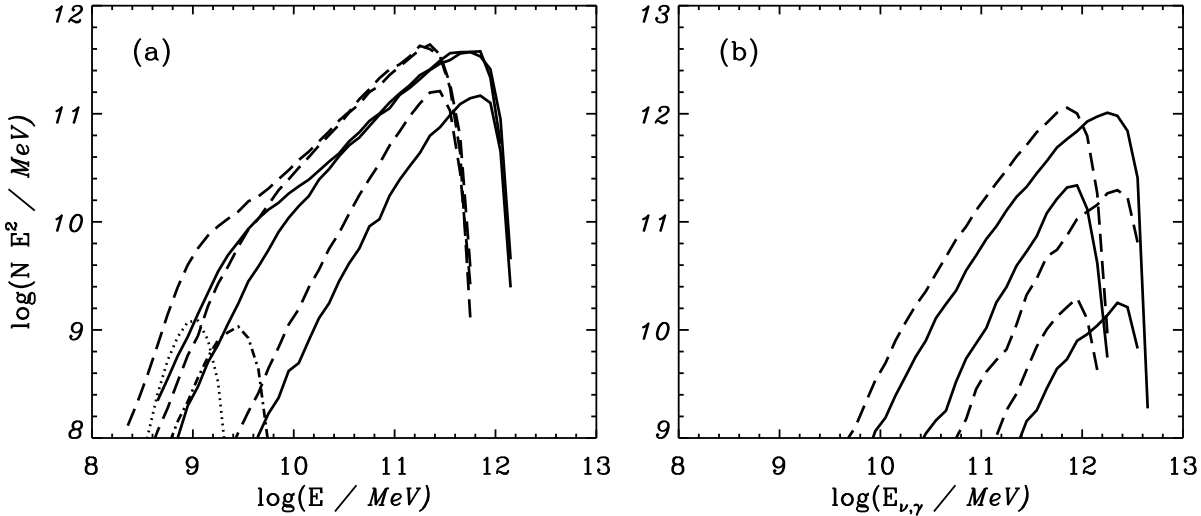


Figure 4. The spectra of γ -rays (full curves) and muon-neutrinos (long-dashed curves) from decay of pions which are produced in collisions of protons with the disk photons. The parameters used are: (a) $T_{\text{in}} = 3 \times 10^4$ K, $l_{\text{rec}} = 10^{12}$ cm (giving $E_p = 3 \times 10^{12}$ MeV); (b) $T_{\text{in}} = 10^4$ K, $l_{\text{rec}} = 3 \times 10^{13}$ cm ($E_p = 10^{13}$ MeV). In each case results are given for $r_{\text{in}} = 10^{14}$ cm (bottom), 10^{15} cm, and 10^{16} cm (top). The dotted and dot-dashed curves in (a) show the spectra of neutrinos and γ -rays for protons with $E_p = 3 \times 10^{10}$ MeV.

where $\gamma_\pi = E_\pi^{\text{LAB}}/m_\pi$, and $\beta_\pi = \sqrt{1 - 1/\gamma_\pi^2}$. The energies of muon-neutrinos from the decay of secondary muons are simply estimated by taking $E_\nu^\mu \approx E_\mu/3$.

The spectra of muon-neutrinos and γ -rays, averaged over the propagation of protons along the direction perpendicular to the disk surface, are shown in Fig. 4. Fig. 4a shows the spectra for the local disk temperature in the region of magnetic reconnection $T = 3 \times 10^4$ K, $l_{\text{rec}} = 10^{12}$ cm, and $r_{\text{inj}} = 1.5r_{\text{in}}$. For these parameters, protons are injected from the reconnection region with energies $E_p = 5 \times 10^{12}$ MeV (see Eq. 10). The full curves show the spectra of γ -rays for the inner disk radii: $r_{\text{in}} = 10^{14}$, 10^{15} , and 10^{16} cm. The corresponding neutrino spectra are shown by the dashed curves. The spectra of γ -rays and neutrinos in the case of protons injected with energies $E_p = 3 \times 10^{10}$ MeV are shown by the dot-dashed and dotted curves, respectively. In Fig. 4b we show the spectra of neutrinos and γ -rays for $T = 10^4$ K, $l_{\text{rec}} = 3 \times 10^{13}$ cm, $r_{\text{inj}} = 1.5r_{\text{in}}$. For these parameters the proton initial energy is $E_p = 10^{13}$ MeV.

3 CASCADE INITIATED BY SECONDARY GAMMA-RAYS

As shown in Figs. 4, the γ -rays originating from decay of neutral pions have extremely high energies. Depending on the conditions above the reconnection region, they can develop cascades in the perpendicular component of the magnetic field via magnetic e^\pm pair production, and subsequent emission of synchrotron photons, provided that their energies fulfill the condition (Erber 1966, B97)

$$\chi \equiv E_\gamma B_\perp (m_e c^2 B_{\text{cr}})^{-1} \geq 0.05, \quad (31)$$

where B_\perp is the component of the magnetic field which is perpendicular to the photon propagation, E_γ is the photon energy, $B_{\text{cr}} \equiv m_e^2 c^3 (eh)^{-1} = 4.414 \times 10^{13}$ G is the critical magnetic field strength, and m_e is the electron rest mass.

For hot disks having weak magnetic fields, the e^\pm pair

energy losses by ICS dominate over synchrotron losses, and the secondary e^\pm pairs initiate ICS e^\pm pair cascades (e.g. Protheroe, Mastichiadis & Dermer 1992, Coppi, Kartje & Königl 1993). In the present work we discuss the case where the magnetic and disk radiation fields are initially in equipartition close to the surface. Therefore the magnetic energy density dominates over the radiation energy density above the disk since the magnetic field drops more slowly with the distance from the disk than the radiation field (Bednarek, Kirk & Mastichiadis 1996b).

The energies of γ -ray photons produced by protons and their distances from the disk on production are stored and used as input to the subsequent cascading in the magnetic field calculated by using the numerical cascade code described in (B97). A sequence of different processes is involved during propagation of these γ -rays. First, the γ -rays cascade in the perpendicular component of the magnetic field above the disk, and we compute the spectra of secondary γ -rays and e^\pm pairs emerging from this synchrotron e^\pm cascade. At distances further from the disk, where the cascade in the magnetic field becomes inefficient, the propagation of γ -rays in the disk radiation is considered. If the inner disk temperature is high enough, some of secondary γ -rays are absorbed creating a second generation of e^\pm pairs. These pairs cool predominantly in the local magnetic field by the synchrotron process, emitting a second generation of γ -rays. Some of the most energetic γ -rays from second generation can further be absorbed in the disk radiation producing tertiary e^\pm pairs which cool by the synchrotron process as well. Since the optical depth for tertiary γ -rays in the disk radiation is low, they usually escape unabsorbed. The emerging γ -ray spectrum is obtained by summing the contributions from all these processes described above. In the present work we use a more general prescription for the dependence of the perpendicular component of the magnetic field along the jet (B_\perp) than applied by Bednarek (B97). Here we use

$$B_\perp(x) = B_0(x/x_1)^{-\beta}. \quad (32)$$

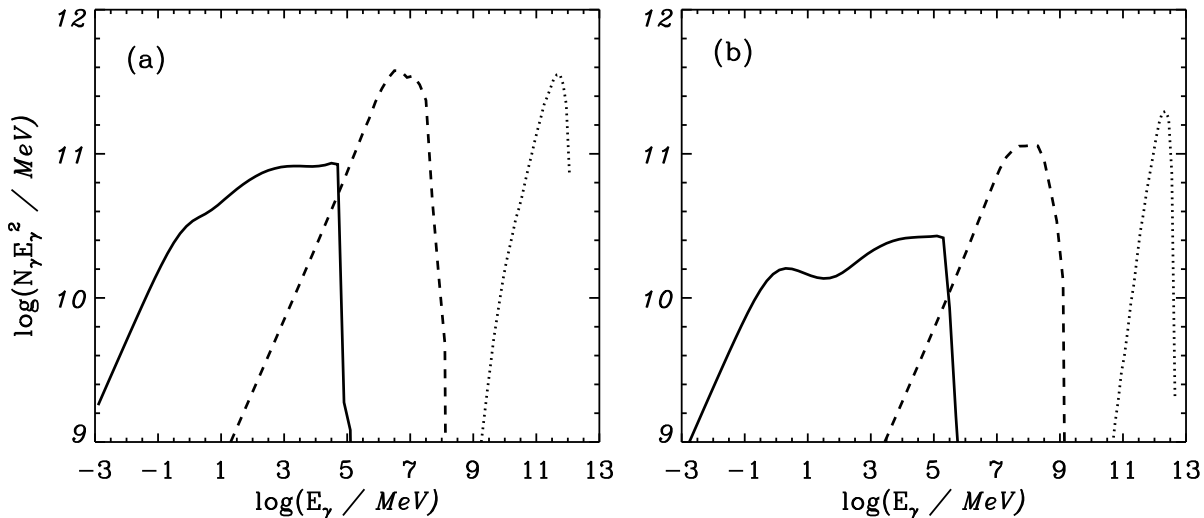


Figure 5. The γ -ray spectra obtained in a sequence of processes, discussed in the text, which are initiated by primary γ -rays produced for the parameters of the model as in Figs. 4(a) and 4(b), respectively, and $r_{\text{in}} = 10^{15}$ cm. The γ -ray spectra from decay of neutral pions produced by protons in collisions with the disk photons are shown by the dotted curves; the γ -ray spectra emerging from the cascade in the magnetic field above the disk are shown by the dashed curves; and the γ -ray spectra from absorption of the cascade γ -ray spectra in the disk radiation, and subsequent synchrotron cooling of secondary e^\pm pairs are shown by the full curves.

which for the cases with $\beta < 1.5$ guarantees that the magnetic energy density always dominates over the disk, radiation energy density above the disk provided that it dominates at the base of the jet (Bednarek, Kirk & Mastichiadis 1996b).

The spectra of γ -rays from the synchrotron e^\pm cascade, and the final γ -ray spectra escaping from the radiation field of the accretion disk, are shown in Fig. 5 by the dashed and full curves, respectively. They correspond to the initial γ -ray spectra from the decay of pions shown in Fig. 4, and for a disk inner radius $r_{\text{in}} = 10^{15}$ cm. In these simulations, we apply the following parameters which define the structure of the magnetic field in the jet above the reconnection region: B_0 is taken to be equal to the value of the magnetic field close to the disk surface, $x_1 = r_{\text{inj}}$, and $\beta = 1.25$. Our simulations show that the shape of the final γ -ray spectrum is not very sensitive to β for values in the range between 1. and 1.5.

4 JUNE 1991 GAMMA-RAY FLARE FROM 3C 279 AND EXPECTED NEUTRINOS

The γ -ray spectra produced in the sequence of processes discussed above are consistent with the spectra observed from FSRQ blazars. As an example, in Fig. 6 we compare the γ -ray spectrum, shown in Fig. 5a, with the observations of the flare from 3C 279 during June 1991 by the COMPTEL, EGRET and Ginga detectors (Williams et al. 1995, Kniffen et al. 1993, Hartman et al. 1996). The accompanying neutrino flare (marked by the dashed curve) corresponds to ~ 28 muon neutrinos per day per km^2 with a typical energy of $\sim 10^8$ GeV. Such a flux, although small, may still be detectable since it is many orders of magnitudes above the neutrino background induced in the atmosphere within the 1° (Lipari 1993) shown by the dot-dashed curve in Fig. 6. The detection probability of neutrino telescopes operating at this energy can be estimated to be $\sim 3 \times 10^{-3}$ (Gaisser,

Halzen & Stanev 1995), giving a rate of ~ 0.1 muons per day per km^2 . Therefore, for typical flares occurring on a time scale of a week one coincident neutrino event should be detected provided that the neutrino is massless. During a period of years, a large neutrino detector should be able to definitively answer the question of the importance of hadronic processes by measurements of correlations between neutrino arrival directions and directions to known FSRQ blazars.

The spectrum of neutrinos expected in this model is limited to a relatively narrow energy range if compared to other hadronic models (e.g. Protheroe 1997, Nellen, Mannheim & Biermann 1993, Mannheim 1995, and comparison of different models in Protheroe 1998). The reason is that we have considered the case in which all hadrons are accelerated in the reconnection region to this same maximum energy, in contrast to other models mentioned in the Section 1, which assumed the injection of a power-law spectrum of protons. Therefore, the shape of the neutrino spectrum may also give us important information on the acceleration mechanism of hadrons in blazars.

5 DISCUSSION AND CONCLUSION

Some models of magnetized accretion disks predict the appearance of relatively small, but efficient, acceleration regions close to the surface of the inner part of the accretion disk as a result of magnetic reconnection (Haswell, Tajima & Sakai 1992, Lesch & Pohl 1992). In this paper, we discuss the consequences of acceleration of hadrons in such regions. Depending on the conditions in the acceleration region, and above the disk (see Fig. 1), accelerated hadrons may either escape, initiate cascades after emerging from the acceleration region, or produce copious secondary leptons during the acceleration process which initiate subsequent leptonic cascading. Primary leptons can also initiate cascades, and this

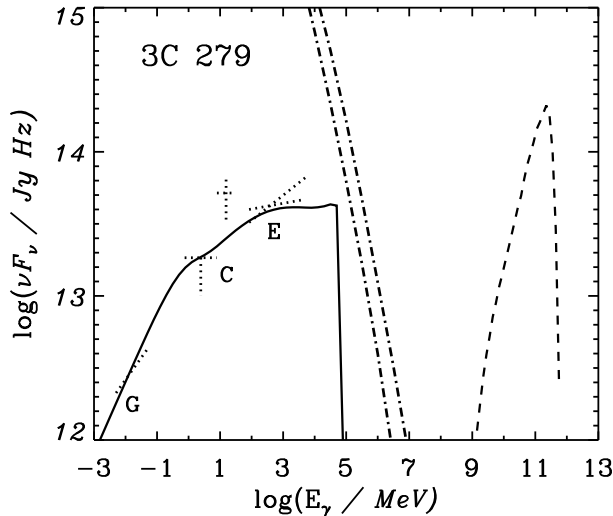


Figure 6. The γ -ray spectrum obtained from the present model (full curve) is compared with observations of the June 1991 flare from 3C 279 detected by COMPTEL (C) (Williams et al. 1995), EGRET (E) (Kniffen et al. 1993) and Ginga (G) (Hartman et al. 1996). The parameters of the fit are as in Fig. 5a. The dashed curve shows the expected muon neutrino flux during this flare. The dot-dashed curves show the atmospheric neutrino background (horizontal - upper curve, and vertical - lower curve) for a neutrino detector with 1° angular resolution.

possibility has been already discussed (B97). In the analysis of hadronic cascades we included the processes of pion production by hadrons, synchrotron radiation of secondary e^\pm pairs in the quantum domain, magnetic e^\pm pair production by γ -ray photons and absorption of the γ -rays in the disk radiation. The γ -ray spectra emerging from such a sequence of processes resemble the spectra observed from FSRQ blazars (Figs 5). Their comparison with the June 1991 flare from 3C 279 allows one to predict the strength of the accompanying neutrino flare (see Fig. 6).

In the present model we have neglected the contribution of interactions of accelerated hadrons with the background matter, either during the acceleration stage, or after propagation through the disk radiation. Interactions of relativistic protons with the disk radiation dominate over the interactions with matter if the density of matter n_H is lower than $n_H \approx 2 \times 10^{11} T_4^3$ particles cm^{-3} ,

$$(33)$$

If the density of matter is relatively high at larger distances from the disk, then protons, at this stage having lost most of their energy during propagation through the disk radiation, can also produce neutrinos by interactions with matter. These neutrinos are typically of lower energies, and their power will be much less than in the higher energy neutrinos from interactions with radiation.

Here we have considered only a single acceleration region in order not to complicate the picture too much. However, in principle many acceleration regions with different parameters could be present simultaneously on the disk surface. Different types of cascades may then contribute to the observed γ -ray spectrum from a specific blazar, and to the neutrino flux. If multiple reconnection sites do contribute, then the neutrino fluxes predicted for a single site should be considered as upper limits. However, a flare being produced

by a single reconnection region seems to be equally probable given the likely short duration of each reconnection region ($\sim l_{\text{rec}}/c$).

It is expected that as a result of magnetic reconnection a large amount of energetic plasma may enter the jet. Therefore, the cascade processes taking place above the reconnection region should also occur in the jet plasma which moves with mildly relativistic speeds. Hence, flares of the type discussed above may be accompanied by additional radiation processes caused by this energetic plasma. Recent multiwavelength observations of Mrk 501 argue that high energy processes in blazars are complicated (see e.g. Pian et al. 1998, Protheroe et al. 1998), and more than one different mechanism may be responsible for producing the observed photon spectrum.

The motion of plasma, and additionally the longitudinal component of the magnetic field in the jet (we do not include its influence on the final γ -ray spectrum) could provide collimation of the produced radiation in the direction perpendicular to the disk surface.

In conclusion, this model predicts that two types of high energy flares may occur if the particles (hadrons, leptons) are accelerated to high energies in reconnection regions on the accretion disk surface. Pure γ -ray flares can be caused either by secondary e^\pm pairs produced during acceleration of protons which collide with the soft disk photons, or by primary leptons accelerated in the reconnection region. In this latter case, the γ -ray spectrum can extend up to TeV energies if the disk temperature is low enough. For large, luminous disks, the magnetic field energy can be efficiently transferred to relativistic protons which can initiate γ -ray and neutrino flares via production of pions in collisions with soft disk photons. Therefore, we suggest that blazars of FSRQ type, for which γ -ray spectra show some evidence of a cut-offs at higher energies (Pohl et al. 1997) and features of large accretion disks (emission lines), may become sources of GeV γ -rays and $\sim 10^{17}$ eV neutrinos. In contrast, BL Lac objects, with spectra extending to TeV energies, should not emit high energy neutrinos according to the present model.

ACKNOWLEDGMENTS

W.B. thanks the Department of Physics and Mathematical Physics at the University of Adelaide for hospitality during his visit. This research is supported by a grant from the Australian Research Council. The work of W.B. is partially supported by the Polish *Komitet Badań Naukowych* grant 2 P03D 001 14.

REFERENCES

- Aharonian, F., Akhperjanian, A.G., Barrio, J.A. et al., 1997, *A&A*, 327, L5
- Bednarek, W., 1993, *ApJ*, 402, L29
- Bednarek, W., 1997, *MNRAS*, 285, 69 (B97)
- Bednarek, W., Kirk, J.G., 1995, *A&A*, 294, 366 (BK95)
- Bednarek, W., Kirk, J.G., Mastichiadis, A., 1996a, *A&A*, 307, L17 (BKM96)
- Bednarek, W., Kirk, J.G., Mastichiadis, A., 1996b, *A&AS*, 120, 571
- Bisnovatyi-Kogan, G.S., Lovelace, R.V.E., 1995, *A&A*, 296, L17

- Blandford, R.D., Levinson, A., 1995, ApJ, 441, 79
- Buckley, J.H., Akerlof, C.W., Biller, S. et al., 1996, ApJ, 472, L9
- Catanese, M., Akerlof, C.W., Badran, H.M. et al., 1998, ApJ, in press
- Chodorowski, M. J., Zdziarski, A.A., Sikora, M., 1992, ApJ, 400, 181
- Coppi, P.S., Kartje, J.F., Königl, A., 1993, in Proc. Compton Gamma-Ray Observatory, eds. M. Friedlander, N. Gehrels & D.J. Macomb (New York: AIP), AIP, v. 280, 559.
- Dermer, C.D., Schlickeiser, R., 1993, ApJ, 416, 458
- Erber, T., 1966, Rev.Mod.Phys., 38, 626
- Gaidos, J.A., Akerlof, C.W., Biller, S. et al., 1996, Nat, 383, 319
- Gaisser, T.K., Halzen, F., Stanev, T., 1995, Phys.Rep., 258, 173
- Ghisellini, G., Madau, P., 1996, MNRAS, 280, 67
- Hartman, R.C., Webb, J.R., Marscher, A.P. et al., 1996, ApJ, 461, 698
- Haswell, C.A., Tajima, T., Sakai, J.-I., 1992, ApJ, 401, 495
- Kniffen, D.A., Bertsch, D.L., Fichtel, C.E. et al., 1993, ApJ, 411, 133
- Lesch, H., Pohl, M., 1992, A&A, 254, 29
- Lichti, G.G., Balonek, T., Courvoisier, T. J.-L., et al., 1995, A&A, 298, 711
- Lipari, P., 1993, Astropart.Phys., 1, 195
- Mannheim, K., 1995, Astropart.Phys., 3, 295
- Mannheim, C., Biermann, P.L., 1992, A&A, 253, L21
- Maraschi, L., Ghisellini, G., Celloti, A., 1992, ApJ, 397, L5
- Mastichiadis, A., 1991, MNRAS, 253, 235
- Matttox, J.R., Wagner, S.J., Malkan, M. et al., 1997, ApJ, 476, 692
- Maximon, L.C., 1968, J.Rev.NBS, 72B, 79
- Nellen, L., Mannheim, K., Biermann, P.L., 1993, Phys.Rev., D47, 5270
- Pian, E., Vacanti, G., Tagliaferri, G. et al., 1998, ApJ, 492, L17
- Pohl, M., Hartman, R.C., Jones, B.B., Sreekumar, P., 1997, A&A, 256, 51
- Protheroe, R.J., 1997, in *Accretion Phenomena and Related Outflows*, IAU Colloq. 163, ed. D.T. Wickramasinghe et al., ASP Conf. Series, Vol. 121, p 585
- Protheroe, R.J., Bhat, C.L., Fleury, P., Lorenz, E., Teshima, M., and Weekes, T.C., 1998, Highlight Paper in Proc. 25th Int. Cosmic Ray Conf. (Durban), in press
- Protheroe, R.J., 1998, in Proc. *Towards the Millennium in Astrophysics: Problems and Prospects*, Erice 1996, eds. M.M. Shapiro and J.P. Wefel (World Scientific, Singapore), in press
- Protheroe, R.J., Mastichiadis, A., Dermer, C.D., 1992, Astropart.Phys., 1, 113
- Romanova, M.M., Lovelace, R.V.E., 1992, A&A, 262, 26
- Shakura, N.I., Sunyaev, R.A., 1973, A&A, 24, 337
- Sikora, M., Begelman, M.C., Rees, M.J., 1994, ApJ, 421, 153
- Stecker, F.W., 1968, Phys.Rev.Lett., 21, 1016
- Stecker, F.W., 1993, in Proc. *5th Int. Workshop on Neutrino Telescopes*, Venice 1993, ed. M. Baldo Ceolin, INFN, 443.
- von Montigny, C., Bertsch, D.L., Chiang, J. et al., 1995, ApJ, 440, 525
- Williams, O.W., Bennett, K., Bloemen, H. et al., 1995, A&A, 298, 33